

## Main Group Element Nets to a T

Andrea Ienco,<sup>†,‡</sup> Davide M. Proserpio,<sup>§</sup> and Roald Hoffmann<sup>\*,†</sup>*Department of Chemistry and Chemical Biology, Baker Laboratory, Cornell University, Ithaca, New York 14853-1301, and Dipartimento di Chimica Strutturale e Stereochimica Inorganica, Università di Milano, Via G. Venezian 21, 20133 Milano, Italy*

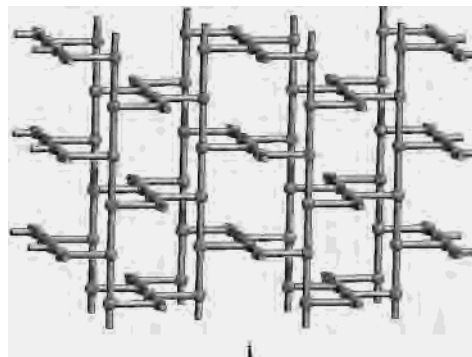
Received November 14, 2003

T-shaped nets (three-coordinated nets with an angular metric, bond angles near 90°, 90°, 180°) are found in a number of extended structures. We explore in this paper the geometrical and electronic consequences of a stricter T-shape metric, where the distances between the vertices of the net are approximately equal and in the range of a chemical bond. Every atom in such a net has a T-shaped environment. One can think of these nets as extensions of BrF<sub>3</sub> or of substructures of various extended tellurium compounds. Several construction principles are found which allow an enumeration of a variety of one-, two-, and three-dimensional T-shape nets; not every three-coordinated net lends itself to the stricter geometrical and distance metric. Not everything is possible; there are no zero-dimensional T-nets, and none made entirely of three atom segments. Previous ideas on electron-rich multicenter bonding lead to a simple way of calculating the magic electron counts for each net; these lie in the range of 6 to 6.67.

## Introduction

Struck by the beauty of a T-shape net (see **1**) observed in some coordination polymers published some years ago<sup>1</sup> (related to a net of a hypothetical carbon allotrope we once studied<sup>2</sup>), and the relationship we saw in it to the T-shape motif found in electron-rich hypervalent bonding chemistry (e.g. BrF<sub>3</sub>), we began thinking about such nets.

The T-shape nets are arbitrarily defined here as a subclass of 3-coordinated<sup>3</sup> nets in which every point of the net has a T-shape environment. The T-shape imposes a metric on a three-coordinated graph; ideally each point of the net has



two 90° angles and one of 180°. Of course, this strict metric constraint can be relaxed and will be in real structures. Until we reach a point in our considerations where geometries are free to relax, wherever we use the term “T-shape net” in this paper we mean the ideal 90°, 90°, 180° net.

Recently some nets of this type have been described.<sup>4,5</sup> These coordination polymers are formed by a metal center linked with an organic spacer, generally a bidentate ligand.

\* Author to whom correspondence should be addressed. E-mail: rh34@cornell.edu.

<sup>†</sup> Cornell University.

<sup>‡</sup> Present address: ICCOM-CNR, Via Madonna del Piano, 50019, Sesto Fiorentino, Firenze, Italy.

<sup>§</sup> Università di Milano.

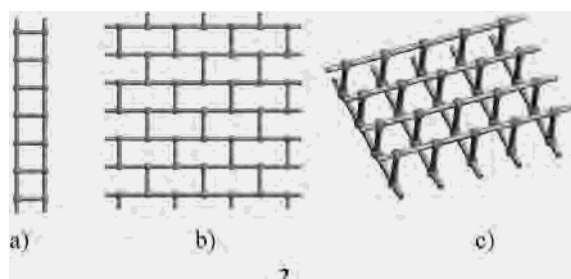
(1) See e.g.: Carlucci, L.; Ciani, G.; Proserpio D. M.; Sironi, A. *J. Am. Chem. Soc.* **1995**, *117*, 4562. Robinson, F.; Zaworotko, M. J. *J. Chem. Soc., Chem. Commun.* **1995**, 2413. Yaghi, O. M.; Li, H. *J. Am. Chem. Soc.* **1996**, *118*, 295.

(2) Hoffmann, R.; Hughbanks T.; Kertesz M.; Bird P. H. *J. Am. Chem. Soc.* **1983**, *105*, 4831.

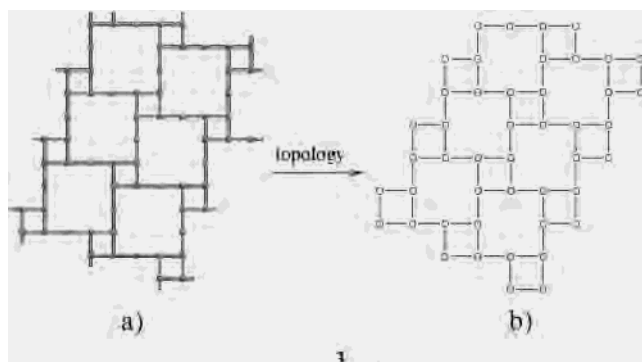
(3) In the initial version of this paper, we used, as chemists usually do, the term “*n*-connected” to indicate the connectivity of a point. Following the suggestion of a referee we consistently changed the word “*n*-connected” to “*n*-coordinated.” This was done in order to avoid a potential misunderstanding with the underlying mathematics, as “connectivity” in graph theory has a different meaning. For a list of basic definitions used in graph theory see: Essam, J. W.; Fisher, M. E. *Rev. Mod. Phys.* **1970**, *42*, 272.

(4) (a) Fujita, M.; Kwon Y. J.; Sasaki, O.; Yamaguchi, K.; Ogura, K. *J. Am. Chem. Soc.* **1995**, *117*, 7287. (b) Losier, P.; Zaworotko M. J. *Angew. Chem., Int. Ed. Engl.* **1996**, *35*, 2779. (c) Hennigar, T. L.; MacQuarrie, D. C.; Losier, P.; Rogers, R. D.; Zaworotko, M. J. *Angew. Chem., Int. Ed. Engl.* **1997**, *36*, 972. (d) Carlucci, L.; Ciani, G.; Proserpio, D. M. *J. Chem. Soc., Dalton Trans.* **1999**, 1799. (e) Dong, Y.-B.; Layland, R. C.; Smith, M. D.; Pschirer, N. G.; Bunz, U. H. F.; zur Loye, H.-C. *Inorg. Chem.* **1999**, *38*, 3056. (f) Jung, O.-S.; Park, S. H.; Kim, K. M.; Jang, H. G. *Inorg. Chem.* **1998**, *37*, 5781.

Scheme 2 shows idealized versions of the different kinds of nets known: (a) 1D ladder,<sup>4</sup> (b) 2D brick<sup>4a,d,5</sup>, (c) a 2D bilayer.<sup>4c,6</sup>



Our interest in the field grew as we imagined building T-shape nets *not* with spacers, but made just of main group elements. What might be the magic electron counts<sup>7</sup> associated with such nets? Aside from the nets shown in **1** and **2**, others are derivable from quite different starting points already in the literature. Thus the Ce<sub>3</sub>Te<sub>22</sub><sup>8</sup> and Ce<sub>4</sub>Te<sub>28</sub><sup>9</sup> phases contain Te sublattices in which some Te atoms have a T-shape environment. **3** illustrates the Te sublattice in the Cs<sub>3</sub>Te<sub>22</sub> crystal. It is made up of small squares of Te atoms linked by a series of 2-coordinated Te atoms. While the 2-coordinated linkage is electronically important, from a topological point of view it can be removed. The sublattice that results (right side of **3**) can then be described as a 2D 3-coordinated net characterized by an equal number of 4- and 8-membered rings.



A metric can specify distances as well as angles. Implicit in the idea of a T-shape net is the assumption that no more than 3 neighbors can be at a “bonding distance” from a net point. For instance the 2D brick (**2b**) and the 2D bilayer (**2c**) nets are *not* good T-shape structures for a net with a main group element atom at *each* vertex (and no “spacer” in between, as in the nets known so far). This follows from the imposition of a distance and angle metric. Without consideration of distances one well might think of a network

such as **2b** and **2c**. But the reality of bonding (e.g. in molecular T-shaped BrF<sub>3</sub>, ClF<sub>3</sub>) points to a maximum bond length differential of ~10% between the two potentially different bonds in the T, and a small deviation of the ideal 90° angles at a point. As we mentioned, we assume in our construction all equal bond lengths in the net, and 90° angles. Given that, in hypothetical **2b** each point has not 3 but 4 neighbors at similar distances and in **2c** each point has 5 neighbors.

In general, we have at hand another, quite chemical, metric, or “topochemical” constraint, a useful way to delimit the number of network possibilities to be considered. Perhaps it is worthwhile to spell out this topochemical constraint, for we will use it often: *If, as a result of translational symmetry and the ideal T-shape constraint, two vertices of a hypothetical net come within a bonding distance (defined as the length of the shortest line connecting two vertices), such vertices will be considered bonded, and a line must be drawn between them.*

In this paper we will examine and classify the possible T-shape nets for main group elements. Our second goal is to calculate the optimum electron count for each net and to obtain some qualitative criteria to judge the stability of the T-shape nets. Before proceeding, it is useful to set out in brief some concepts for characterizing the nets.

### Gons and Vertices: The Classification of the 3-Coordinated Nets

A net is made up of points or vertices, joined by links (bonds). A way to describe nets is in term of their circuits (polygons, or, in a chemical language, rings) and the coordination or number of linkages of the vertex (degree in the graph theoretical terminology).<sup>10</sup> We are interested in uniform infinite lattice graphs, uniform meaning that each vertex has the same degree (3 in our case). We divide the T-shape nets into two categories: “planar” nets if the nets lie in a Euclidean space plane; otherwise we call them “nonplanar”.

For the 2D planar nets, we use in our paper the language (and most conventions) of Wells. A net can be identified by the number (*n*) of the smallest polygons of all independent links. In the brick net (**2b**) the smallest rings are all hexagons, while the net in **3b** is formed by two different kind of squares, a 4-membered square (or 4-gon) and an 8-membered square (or 8-gon). Note right away that we use the word “square” as a geometrical descriptor and *not* the equivalent of “4-gon”. The ideal 4-gon is square, but so is an 8-gon that will be of great interest to us.

The other quantity is the number (*p*) of links meeting at each vertex. The notation is (*q*, *p*) where *q* is the *n*-gon size (the number of edges making it up) and *p* was defined above. The brick net (**2b**) is described as (6, 3) where 6 is the number of edges of all the smallest rings and 3 is the degree of the vertices.

(5) Gudbjartson, H.; Biradha, K.; Poirier, K. M.; Zaworotko, M. J. *J. Am. Chem. Soc.* **1999**, *121*, 2599.

(6) (a) Kondo, M.; Yoshitomi, T. Seki, K.; Matsuzaka, H.; Kitagawa S. *Angew. Chem., Int. Ed. Engl.* **1997**, *36*, 1725. (b) Power, K. N.; Henningar, T. L.; Zaworotko, M. J. *New J. Chem.* **1998**, 177.

(7) Papoian, G. A.; Hoffmann, R. *Angew. Chem., Int. Ed.* **2000**, *39*, 2408.

(8) Sheldrick, W. S.; Wachhold, M. *Angew. Chem., Int. Ed. Engl.* **1995**, *34*, 450 Kanatzidis, M. G. *Angew. Chem., Int. Ed. Engl.* **1995**, *34*, 2109.

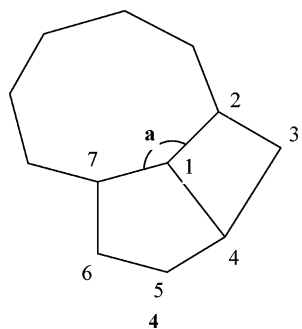
(9) Sheldrick, W. S.; Wachhold, M. *Chem. Commun.* **1996**, 607.

(10) (a) Wells, A. F. *Three Dimensional Nets and Polyhedra*; Wiley: New York, 1977. (b) Wells, A. F. *Further Studies of Three-dimensional Nets*; ACA Monograph 8; American Crystallographic Association: Buffalo, NY, 1979.

If there is more than one kind of smallest circuit, as for instance in the case of the net shown in **3b**, the symbol becomes  $(n^x.m^y.l^z \dots, p)$  where  $x, y, z$  are the number of circuits of length  $n, m, l$ . So the symbol for **3b** is  $(4^1.8^1, 3)$  or  $(4.8, 3)$  if we drop the exponent when it is 1.

This representation is in general insufficient to identify uniquely a net, so it may be also necessary to specify other characteristic. Following the notation of Wells, these may be  $Z_i$ , the number of points in the smallest topological unit cell,  $^n x$ , the number of rings to which a vertex belongs, and  $^n y$ , the number of  $n$ -gons to which a link belongs. Sometimes even larger circuits must be specified.

In general, as shown by O’Keeffe,<sup>11,12</sup> the topological classification and the enumeration of the nets is still an open and unresolved problem. A useful notation for the nonplanar nets is the vertex symbol (also called long Schläfli symbol). It records the shortest rings linking each kind of vertex in the net. A 3-coordinated net has 3 different angles associated with a vertex, and the symbol for the vertex has the general formula  $(Q1_A.Q2_B.Q3_C)$  where  $Q1, Q2,$  and  $Q3$  are the shortest “ring” size associated with the angle 1, 2, and 3 respectively and  $A, B, C$  are the number of the shortest ring. “Ring” is meant here in a chemical way; in general it may happen that the shortest circuit does not correspond to the shortest ring, as shown in **4**. For the **a** angle, the 7-membered circuit contains the shortcut 1–4, and so in this case the shortest ring is the 8-membered one.



Also the vertex symbol is sometimes unable to differentiate two networks and we have to consider other parameters, such as the “coordination sequence”. The locally modified program EUTAX helped us in the topological analysis of the nets.<sup>13</sup>

For the sake of simplicity, we will use a code to identify a network. The format of the code is “**XD-qx**”. The first part, “**XD**”, refers to the dimensionality of the net; it can be **1D, 2D,** or **3D** for nets infinitely extended in one, two, or three dimensions, respectively. In principle, **XD** could be **0D**, but with a T building block it is not possible to make a finite net. The “**q**” in the code is “**p**” (for **p**lanar) when the net lies in a plane, or it can be “**n**” (for **n**onplanar) when the net is nonplanar. The last letter “**x**” is just a counter, an enumerating index.

(11) O’Keeffe, M.; Hyde, B. G. *Crystal Structures I. Patterns and Symmetry*; Mineralogical Society of America: Washington, DC, 1996.

(12) O’Keeffe, M. Z. *Kristallogr.* **1991**, *196*, 21.

(13) O’Keeffe, M. EUTAX, local modified PC version by D. M. Proserpio.

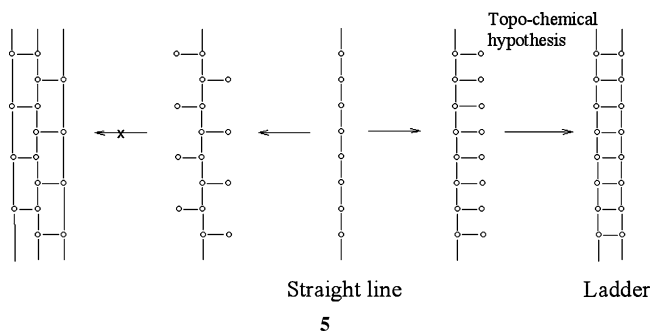
We need to stress that our code is just a way for enumeration of the nets we found, and there is no direct relation with the mathematical topology of the nets. In general, we can have nets with the same topological description but with different arrangement in the space.

The Supporting Information to this paper gives for every net discussed the unit cell constants, coordinates of points, space group, densities, and vertex and Wells (when applicable) symbols.

## 1D Planar Net

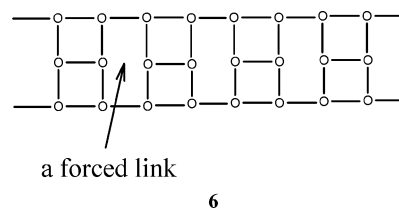
Let us now begin to construct some ideal T-shape nets, proceeding from one dimension to three. The simple ladder, **1D-p1** (see **2a**), is the only planar 1D T-shape net compatible with our topochemical hypothesis. Though this is obvious, it is useful to show the reasoning, for it will be applied soon in a more complex setting.

We begin with a straight line, which incorporates the necessary translational symmetry. The points in the straight line (middle of **5**) are 2-coordinated and have to be linked with another one. One option is to put the third point of each T to the same side of the straight line (right of **4**). Let us take a look at the environment of these atoms. The two neighbors of each atom are at a bonding distance, which, by the topochemical hypothesis, leads to a bond between them. This is fine, we have a 1D T-shape net, the ladder.



An alternative, shown in **5** (left), is to alternate the third link as one translates along the line. But this leads to an unacceptable geometry—a closure would be required with two bonds twice as long as the original point separation along the central line. There are also other possibilities, but all of them lead to similar problems.

To stress again the importance of the topochemical hypothesis in the generation of our nets, we show in **6** another hypothetical 1D solution. It actually is 4-coordinated; the arrow points to the region where a bond is forced.



## 2D Planar Nets

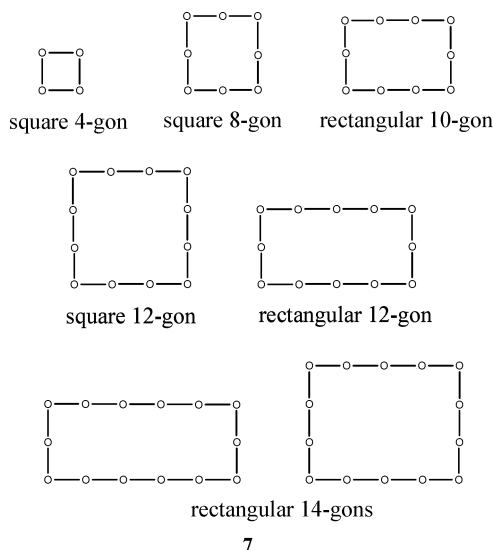
2D 3-coordinated plane nets have been studied extensively and elegantly by Wells,<sup>10,14</sup> as well as by others.<sup>15</sup> Wells has

developed a formalism for labeling and enumerating them. He shows that the 3-coordinated 2D plane nets conform to the following equation, where  $\sum \phi_n = 1$  and  $\phi_n$  is the fraction of the total number of polygons that are  $n$ -gons:

$$3\phi_3 + 4\phi_4 + 5\phi_5 + 6\phi_6 + 7\phi_7 + \dots + n\phi_n = 6 \quad (1)$$

For instance, in the honeycomb net of graphite all  $\phi$ 's are zero except  $\phi_6 = 1$ . In (4.8, 3), in the net made of squares and octagons in scheme **3b**,  $\phi_4 = 1/2 = \phi_8$ . O'Keeffe showed that eq 1 can be derived from the Euler relationship between the number of vertices, the number of polygons, and the number of edges ( $V + P = E$ ).<sup>15</sup>

In the sometimes complex argumentation that follows, it is important to make explicit the constraints of the T-shape, and a possible confusion in language. We will use consistently the words 4-gon, 8-gon, 10-gon, etc. for polygons. But the T-shape constraint dictates angles of 90° and 180°. Thus the 8-gon built of T-shapes (and higher  $n$ -gons) is *never* the regular octagon, with all angles equal; only rectangle or square-shaped 8-gons are possible in T-shape nets. Examples are given in **7**.



We emphasize again that we use “square” as a geometrical descriptor, not as equivalent to a 4-gon, though our 4-gon is, in fact, a square. We can also have different shaped polygons. As shown in **7**, the 12-gon can take on a square as well as a rectangle geometry and the 14-gon can have two different rectangular shapes. By the way, **7** describes all the possible planar shapes for 4-gon through to 14-gon, assuming only 90° or 180° angles (as is required to build a T-shape net). This will be important for the net generation algorithms we will develop.

The Wells equation can be simplified in our case. With a T-shape building block we can form only square or rectangular circuits, since the angles can be only 90° or 180°. In a rectangle or square the perimeter must be  $n$  times the length of the repeating unit, because we impose the condition that

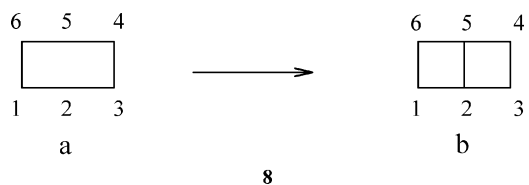
**Table 1.**  $m$  “Order”: The Highest Denominator in  $\phi_n$ ;  $Z$  the Number of Points in the Repeating Unit;  $\phi_n$  the Fraction of the Total Number of Polygons That Are  $n$ -Gons

$m$	$Z$	$\phi_4$	$\phi_8$	$\phi_{10}$	$\phi_{12}$	$\phi_{14}$	$\phi_{16}$	net type
2	4	1/2	1/2					<b>2D-p1</b>
3	6	2/3		1/3				<b>2D-p2, 2D-p6</b>
4	8	3/4			1/4			<b>2D-p3, 2D-p7</b>
5	10	3/5	1/5	1/5				<b>2D-p10</b>
5	10	4/5				1/5		<b>2D-p4, 2D-p8</b>
6	12	4/6	1/6		1/6			<b>2D-p11</b>
6	12	5/6					1/6	<b>2D-p5, 2D-p9</b>

all the linkages have equal length. Furthermore, in a square and a rectangle  $n$  is even (the opposite sides have to be of the same length.). Equation 1 becomes

$$4\phi_4 + 6\phi_6 + 8\phi_8 + 10\phi_{10} + \dots + 2n\phi_{2n} = 6 \quad (2)$$

Also the term that represents the six-member ring in eq 2 has to be dropped, as a consequence of our topochemical hypothesis. Only one kind of *planar* rectangle can be formed with a six-member circuit, as may be seen from **8a**. But, as shown in **8b**, the “topochemical” hypothesis makes one add a link between points 2 and 5, and this transforms the six-point rectangle into two four-point squares.



The final form of the eq 1 applicable to our T-shape nets is

$$4\phi_4 + 8\phi_8 + 10\phi_{10} + \dots + 2n\phi_{2n} = 6 \quad (3)$$

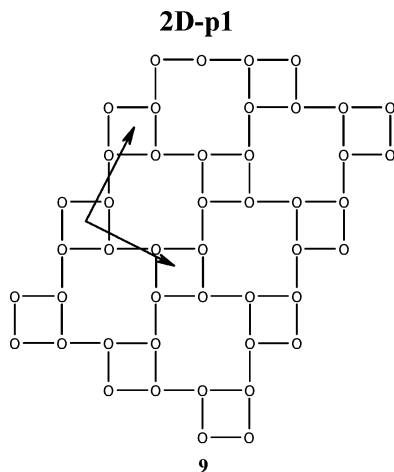
One consequence of eq 3 is that we cannot have a 2D planar T-shape net with all polygons of one kind; also the nets must contain at least *one* 4-member square. There are an infinite number of solutions of eq 3. However, we are interested in nets with a small number of nonequivalent circuits and with a pattern of vertices that repeats periodically with a “reasonably” small unit cell. In Table 1 we report the nontrivial solutions of eq 3 from  $m = 2$  to  $m = 6$  where  $m$  (order) is the highest denominator of  $\phi_n$ .

Let us describe the nets that correspond to these solutions. The first one, **2D-p1**, is shown in **9**, and belongs to the (4.8, 3) family of nets, using the convention of Wells. This is the only T-shape net we can build with only 4- and 8-gons. This is important, because (as Wells showed<sup>14</sup>), without the topochemical and angular metric conditions we impose, an infinite number of (4.8, 3) nets can be constructed. The proof is given in the Supporting Information.

We now show the nets associated with the other solutions of eq 3, starting with the nets with only two kinds of gons. For these solutions, there are two different ways for assembly of the gons. The first assembly is shown in **10**. The nets **2D-p2**, **2D-p3**, **2D-p4**, and **2D-p5** are characterized by straight lines and ladders connecting them. The vectors in the drawing indicate a unit cell.

(14) Wells, A. F. *Acta Crystallogr.* **1968**, B24, 50.

(15) O'Keeffe, M.; Hyde, B. G. *Philos. Trans. R. Soc. London* **1980**, 295, 553.



In the second family of nets (see **11**), there are no more straight lines, but a different assembly of the ladders. It may be noticed that the **2D-p1** net is also a member of this family. In fact, the other nets can be viewed as an expansion of the 8-gon square of the **2D-p1** net.

The two nets obtained from the third solution of eq 3 are shown in **12**. The **2D-p10** lattice is a variation of the **2D-p6** family. Ribbons containing 10-gons and ribbons containing 8-gons alternate in an *ABAB* fashion. Obviously we can obtain an infinite number of nets just varying the order of the ribbons (i.e. in *AABB* sequence). The **2D-p1**, **2D-p3**, and **2D-p11** nets are built using only squares.

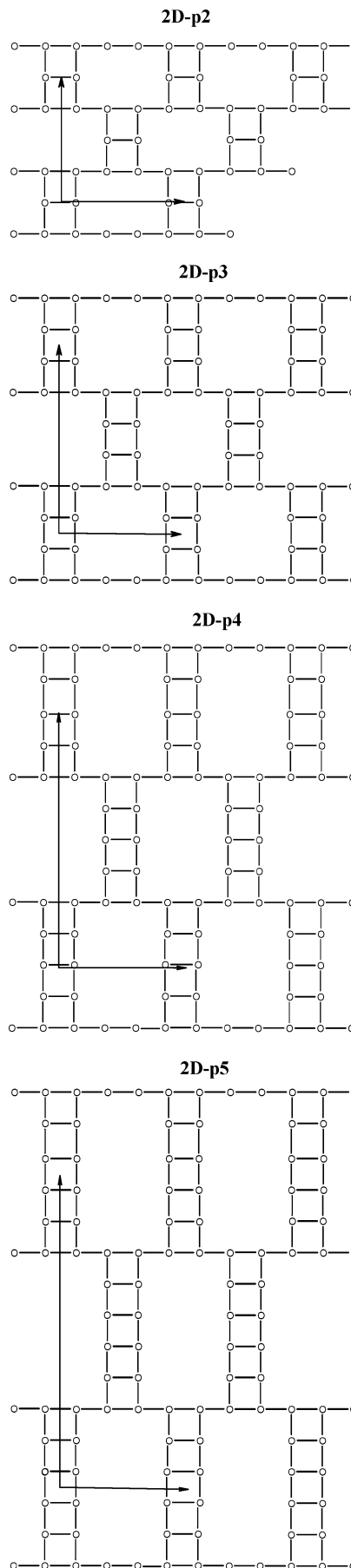
As one looks at the totality of the nets generated so far, it becomes clear that they may be all viewed as derived from a simple square-planar grid through the removal of points. This observation gave us another method for net generation (how many ways are there of removing points from a square net so as to leave *each* remaining vertex 3-coordinated?) as well as a simple way for calculating the atom density of a given structure.

### Nonplanar Nets

Our starting point for the generation of 3D nets is the Wells enumeration.<sup>10</sup> He described in his classic and insightful book<sup>10a</sup> 30 3-coordinated nets with only one kind of polygon and some others with 2 different kinds of circuits. Our idea was to superimpose the ideal T-shape metric on Wells's set. It turns out that not all of the Wells nets can be reduced to T-shape nets. Our own enumeration is not exhaustive, but it aims to show all the possible T-shape nets that have small unit cell, high symmetry, and high density. Important sources for us, aside from the Wells books,<sup>10</sup> were the book of O'Keeffe and Hyde<sup>11</sup> and the enumerations of Koch and Fischer<sup>16</sup> and of Bader, Klee, and Thimm.<sup>17</sup>

### Nonplanar 1D Nets

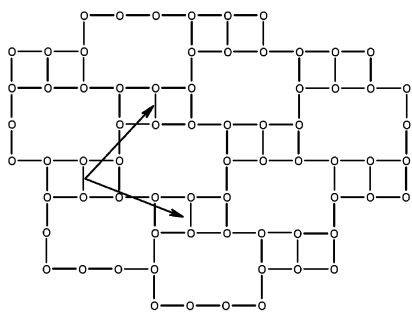
In this section we deal with the nonplanar 1D structures. The first 1D nonplanar net is strictly related to the **1D-p2** family. To build the net, we first take a ribbon of the **1D-p2** net with 4 straight lines and four ladders, as shown in **13**.



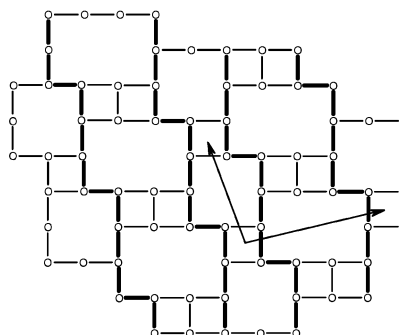
(16) Koch, E.; Fischer, W. *Z. Kristallogr.* **1995**, *210*, 407.

(17) Bader, M.; Klee, W. E.; Thimm, G. *Z. Kristallogr.* **1997**, *212*, 553.

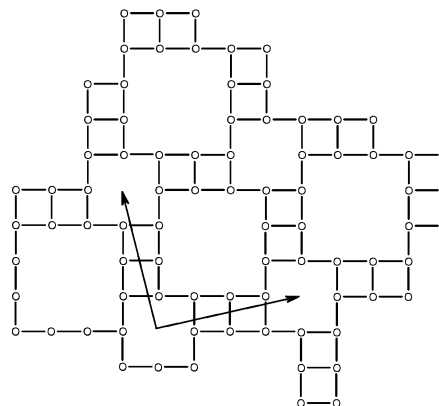
2D-p6



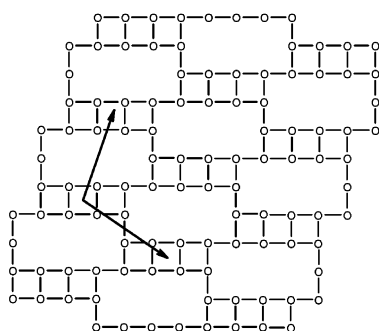
2D-p10



2D-p11



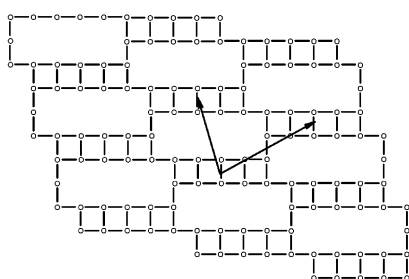
2D-p7



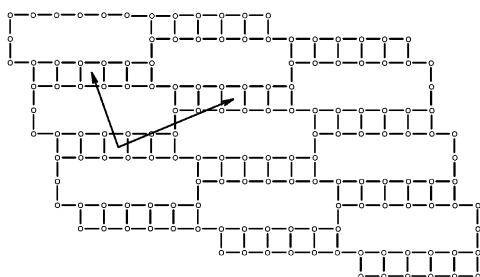
12

Folding the ribbon into a tube, we obtain the **1D-n1** net (see **14**). This folding in fact does not destroy the local T-shape geometry of the points. This is a construction principle of some utility.

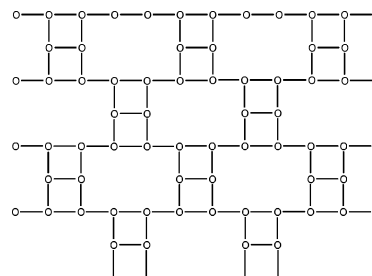
2D-p8



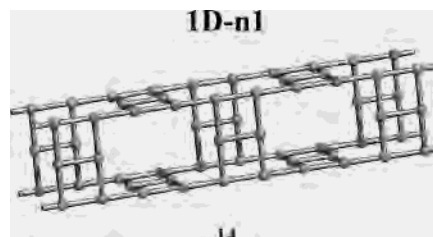
2D-p9



11



13

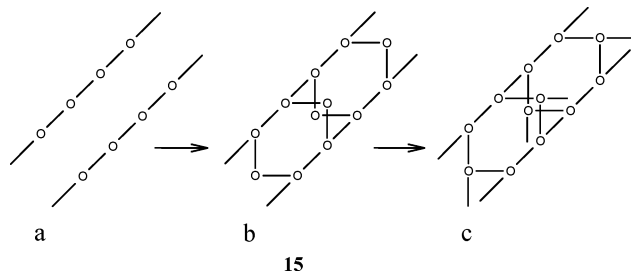


14

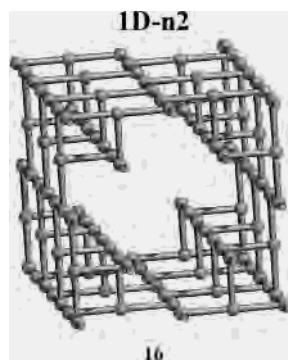
Just varying the number of the straight lines and/or the height of the ladder in between, we can generate an infinite number of such tubes as well as an infinite number of 2D and 3D nets (not shown here). The only constraint concerns the number of the tube faces. It has to be even, otherwise it is not possible to close the tube.

The tube **1D-n1** is not a rigid one and can be deformed from the square arrangement to a rhomboidal one, or even (unrealistic) squashed flat. A material, built using this spatial arrangement, should in principle show a negative compressibility in one direction when hydrostatic pressure is applied.<sup>18</sup>

Another family of 1D nets can be built in this way. Let us take two parallel straight lines, and connect them as shown in **15**.



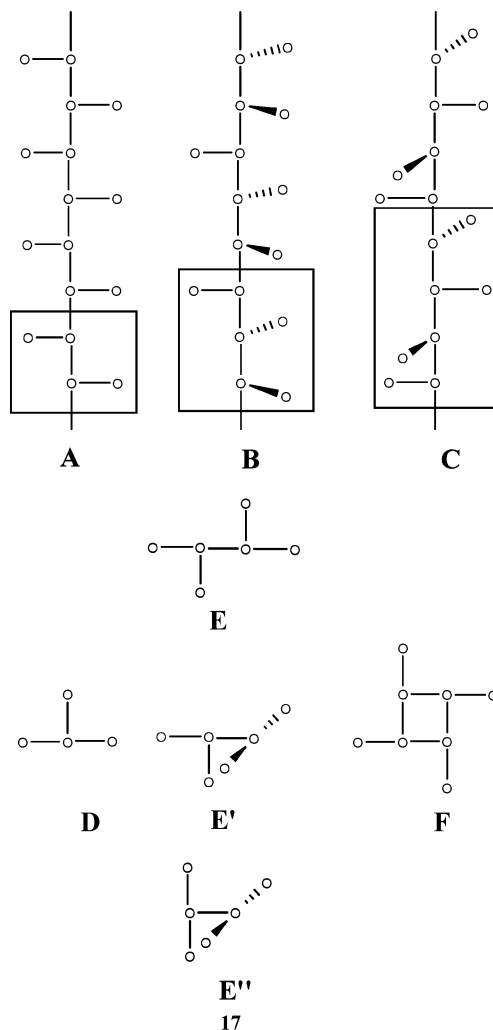
While the vertices of the two straight lines are T-shape, the other vertices are 2-coordinated. We can link the latter with other points, as indicated schematically in structure **15c**. With 4 such building blocks we can make the **1D-n2** tube (see **16**). In this family we can only build tubes with an even number of building blocks. Also connecting in different ways the building block **15c**, an infinite number of 2D and 3D networks can be obtained.



### Building Blocks

Before starting with the enumeration of more complex structures, we think it is useful to introduce the concept of building blocks. These will help us to describe the structures, and the reader to visualize them. The building blocks are geometrical entities that we found making up the 2D and 3D structures. Scheme **17** introduces the building blocks.

The first building block, A, is a straight line of points with bonds alternately along two different directions. The “B” and the “C” straight lines are related to A; the bonds are repeated after three and four turns, respectively. In general the building blocks “A”, “B”, and “C” can define a crystallographic screw axis only when the dihedral angles between the arms are 180°, 120°, and 90° in building blocks “A”, “B”, and “C”, respectively. A simple 3-coordinated point is the building block “D”. The “E” series of blocks are three different ways of linking two T-shape points. The straight line A also can



be reduced to an infinite link of E blocks. The last block we use is the “pinwheel” F.

The use of building blocks is a practical way of describe and think of the T-shape structures, not a way to classify them. This tool allows us to build T-shape nets from scratch or reduce already described nets in the literature (see below). Another advantage will be in the calculation of the electron count of the nets. Now let us start with the description of the other nets.

### Nonplanar 2D Nets

A useful way of introducing the 2D nets is to divide them into two categories: layered nets and nonlayered ones. The first two nets (**2D-n1** and **2D-n2**) belong to the second type. Both of them are built using A and E blocks, as highlighted in Figure 1. The difference between the two nets shows up in the projection along the cell axis. For **2D-n1** the projection shows a series of squares linked by a segment, for **2D-n2** instead a condensation of rectangles.

The bilayer net **2D-n3** can be described as formed by E' and D blocks as illustrated in Figure 1. The reader may have also noticed that there are other ways to describe it (i.e. using the C line and E'' block or E' and E'' blocks). As an alternative (see **18**), the net can be built from the addition of 2-coordinated atoms between the points of a brick net

(18) Baughman, R. H.; Stafström, S.; Cui, C.; Dantas, S. O. *Science* **1998**, *279*, 1522.

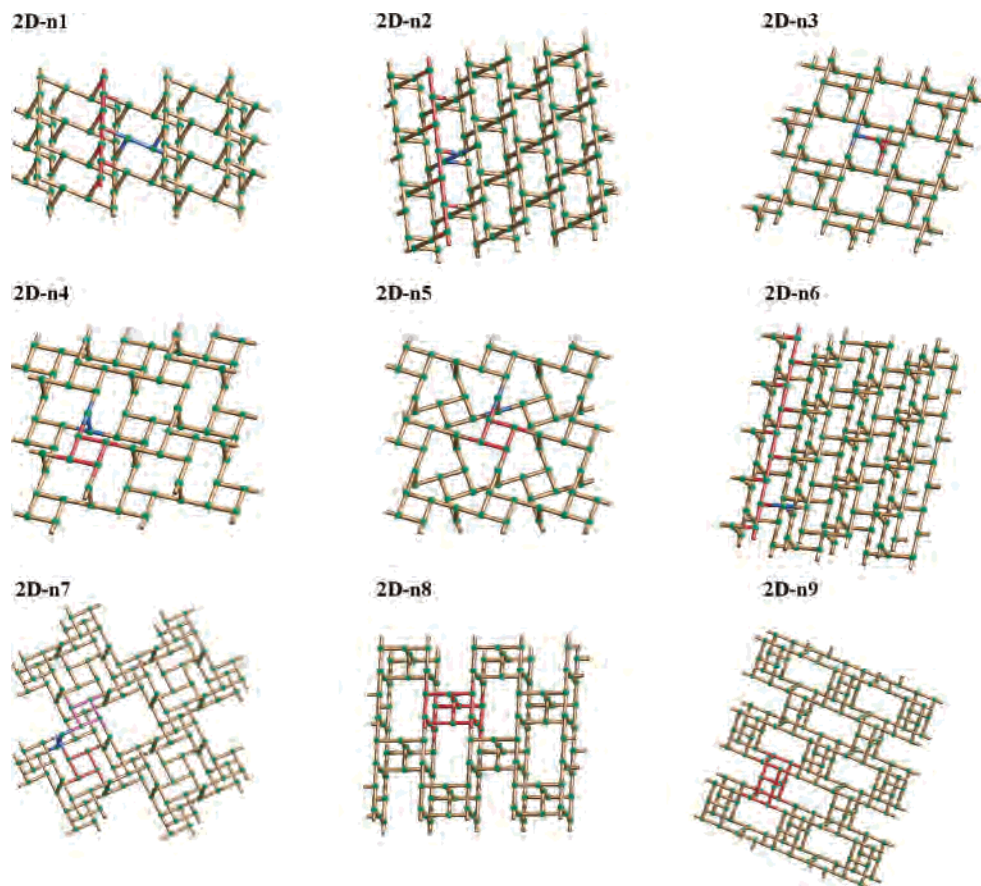
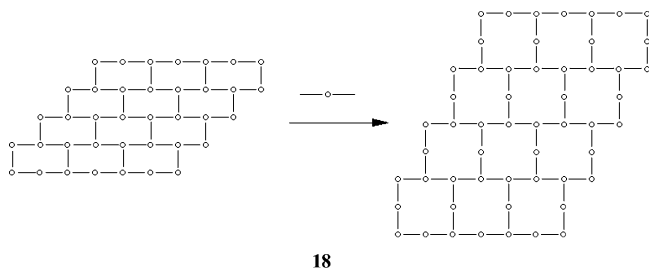


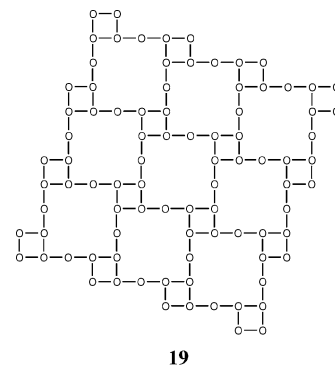
**Figure 1.** A view of the 2D nets. The building blocks are highlighted with different colors.

(2b). The 2-coordinated points are linked with the 2-coordinated points of a similar brick net rotated by 90°. Notice that the shortest circuit in this net is a 6-gon. This is possible because we are not any more in a plane. Nonplanar 6-gons are consistent features of 2D and 3D T-shape nets.



Two other bilayers are **2D-n4** and **2D-n5**. Both of them can be assembled using the F square and E' blocks. It also may be useful to consider them formed from two real  $\text{Te}_6$  sublattices of  $\text{Cs}_3\text{Te}_{22}$  (see **19**) connected through the 2-coordinated vertex. In **2D-n4** the two planes have the same direction while in the other case they are rotated.

Aside from their intrinsic interest, these two nets tell us that two T-shape nets can be identical in connectivity as well as topologically, but have quite a different geometrical arrangement. And maybe these nets are not so remarkable. Each component net (the  $\text{Cs}_3\text{Te}_{22}$  net, **19**) is characterized by a 4-fold symmetry axis and no planes. The assemblage of two such units generates two nets **2D-n4** and **2D-n5** that



are related topologically, but not identical. And they are not superimposable in Euclidean space. Such should also be distinct electronically, due to the different environment of atoms in each.

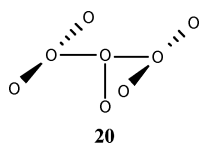
When we started to analyze the nonplanar nets, we thought that we could build all of them in a way analogous to the planar nets, using a cubical six-coordinated grid and removing points from it. It is now obvious that this method can generate some nets but not all, as **2D-n4/n5**, obvious exceptions, tell us.

**2D-n6** is a three-layer net, assembled using A lines and points D. Another way to describe the net is the following: The first and the third layers have the same pattern, but in the final assembly they are shifted by one position in a perpendicular direction. Parallel straight lines constitute the middle layer. In this net all the smallest rings are 8-gons (as

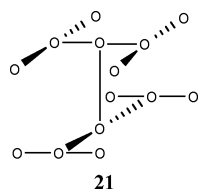


for **2D-n2**). In the next section we show that this net is closely related with the **3D-n5** net.

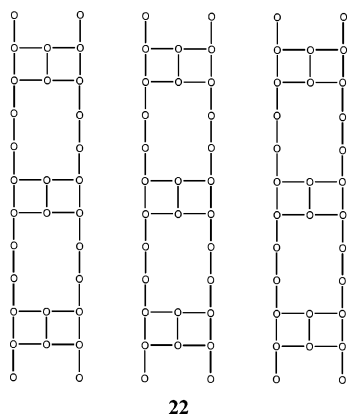
The next net, **2D-n7**, is again a three-layer one. It is easy to recognize in it the F square block, while the second element (see **20**) can be considered formed by three D points linked together. It shares many common features with the **2D-n4** and **2D-n5** nets. As in these nets, the upper layer of **2D-n7**, as well as the central layer (highlighted in red in Figure 1), can be rotated with respect to the bottom one, forming two other different geometrical rearrangements without modifying the topological description of the net. Moreover each square of the central layer can be rotated independently of the other ones, obtaining an infinite number of different and less symmetric nets.



The top view of the last net we present in this section, **2D-n8**, shows the same pattern as the **2D-p2** net. At a first sight **2D-n8** seems also related to the **1D-n1** family of nets. In reality, the linkages between the straight lines are made using two **20** building blocks bonded together as shown in **21**.



A slight modification of **2D-n8** is the three-layer **2D-n9**. It is built joining together two planes of the type shown in **22** with the building blocks of **21**. Obviously the top view of **2D-n9** is the same as that of **2D-n8**.



It is interesting to notice that **2D-n7** and **2D-n8** can expand in the third direction. For **2D-n7**, a 3D net can be built shifting up some of the building blocks of type F to connect to an upper layer (not shown here). The same trick can be used for the building block shown in **21** for the **2D-n8** net (see later **3D-n16**). In contrast to **2D-n7**, the growth of the

**2D-n8** net in the third dimension can be stopped by capping the net with two planes of the type shown in **22**.

In principle, we can build nets with a number of layers varying from 3 to  $3n$ , where **2D-n9** is the first member of the series. Notice that if we use just one plane **22** we can obtain a semi-infinite net.

### Infinite 3D Nets

The 3D nets we have found are shown in Figure 2. The building blocks are highlighted with different colors to facilitate the representation of the structure.

First of all, we want to show the nets built by using only one type of block. The simplest one is the **3D-n1** net. It is the net from which all of this work began. The net can be obtained by connecting, in an *abab* sequence, two parallel planes. In the first plane a set of A straight lines is parallel to the crystallographic *a* direction, a second set with the *b* direction. Wells described this net as (10,3)-b.<sup>10a</sup> The topology of this net is the same of the silicon atom sublattice of the  $\text{ThSi}_2$  crystal. This net, as well as the **1D-n1**, can be deformed from a tetragonal configuration to a rhombic one without breaking the T-shape nature of the points.

The **3D-n2** net is closely related to the latter and was described by Wells as (10,3)-c.<sup>10a</sup> Also in this case, this net has the topology of the boron atom sublattice in the  $\text{B}_2\text{O}_3$  net. In this case there are three planes of straight lines A, each rotated by  $120^\circ$ . In Figure 2, the three sets of planes are colored in green, red, and yellow. This net cannot be deformed and is rigid.

The **3D-n3** net is formed by assembly of C blocks. Three sets of such lines are disposed perpendicularly to each other, as shown in Figure 2. In this case, the three projections of the net are equivalent, and the net is characterized by square channels, alternating with straight lines of atoms. The smallest circuit in this net is a six-membered one.

The last net we are able to build using only one type of building block is **3D-n4**. It is assembled using only the F blocks. The net is derived through a series of nonobvious transformations of the (4,12<sup>2</sup>) net described by Wells. The density of **3D-n4** (0.316) is the lowest of all the structures we have presented in our enumeration. **3D-n4** is also the only 3D net without infinite lines.

The next four nets are built using the D block alternated with A, B, and C blocks. Topologically, **3D-n5** and **3D-n6** come from the Wells (8,3)-c net. Their A building blocks are connected in different way, as can be seen from the *c* projection of the two nets (see Supporting Information). Interestingly, the **3D-n5** net can also be constructed by alternating the two external layers of **2D-n6** with two layers of straight lines.

The **3D-n7** net is special. From the top, it appears to be made up of equilateral triangles and irregular hexagons. The B building blocks are at the vertices of a triangle. Interesting 3-fold screw axes are present as symmetry elements, but they are not coincident with the building blocks and are located at the center of the triangles. The dihedral angles between

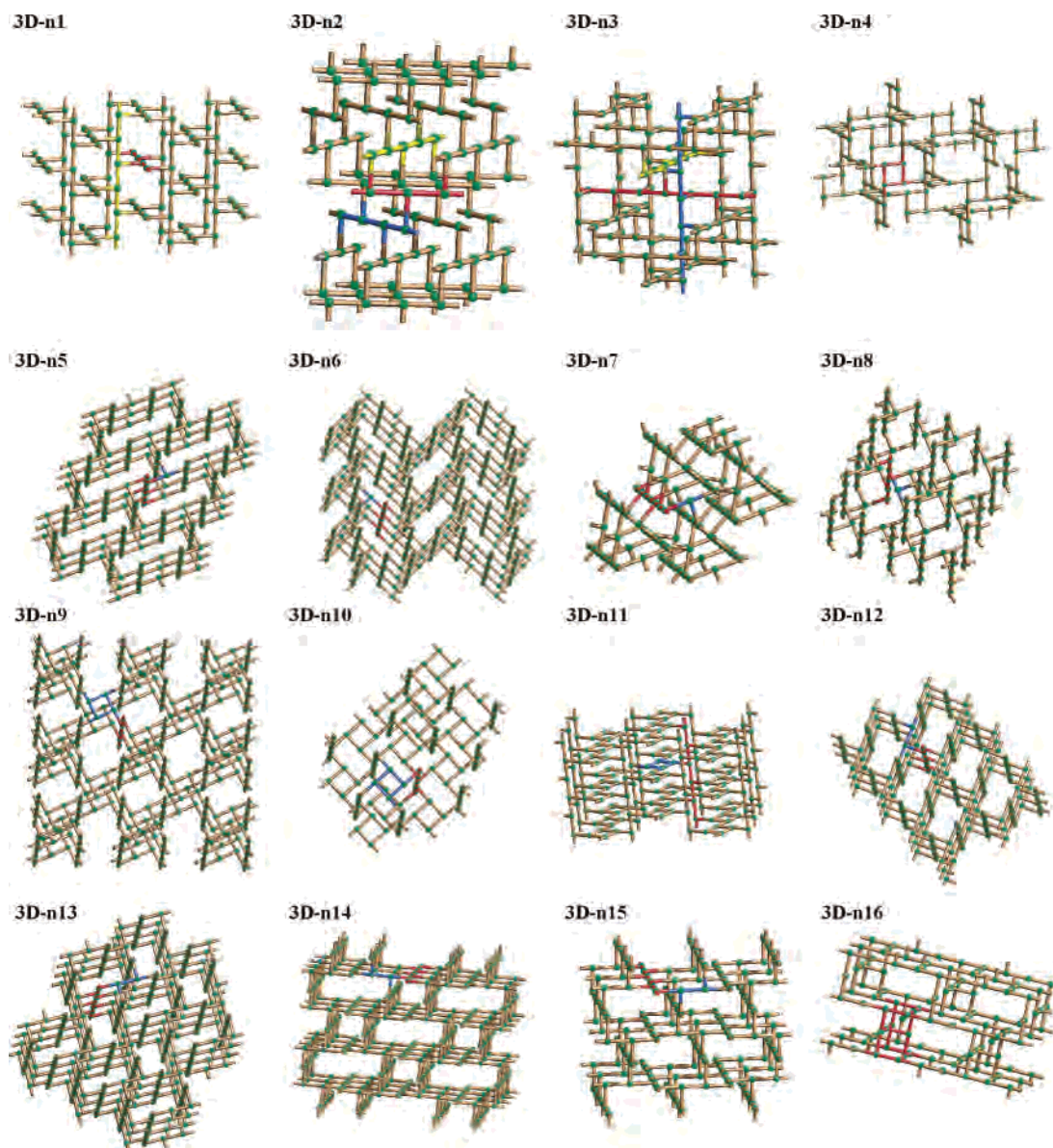


**Figure 2.** A view of the 3D nets. The building blocks are highlighted with different colors.

the arms of the B building block are  $120^\circ$ ,  $60^\circ$ , and  $120^\circ$ , respectively. It is quite incredible that this net may be derived from the Wells (10,3)-a net, and consequently has the same topological description. Also the silicon atom sublattice in  $\text{SrSi}_2$  has this topology.

Using the 4-fold building block C, we built the **3D-n8** net. At first sight, this net appears to be related to **3D-n3**, especially looking at the projection along the *c* direction. In both nets the smallest circuit is a 6-gon, and both are characterized by square channels. On the contrary, the **3D-n8** has the channels only in the *c* direction and a different topology description.

The next three nets (**3D-n9**, **3D-n10**, and **3D-n11**) are assembled by putting together the square block F and B or C lines. **3D-n9** is characterized by large square channels along the *c* direction, while in **3D-n10** there are large voids. The importance of these structures is due to the presence of a large number of triatomic straight segments, a feature that

will emerge as critical when we turn to electron counting. In **3D-n11** the square blocks are joined together. This net was obtained by modifying the net called 6(3)3-26 of ref 17. Obviously, as in the case of **2D-n4** and **2D-n5**, other nets isomeric to **3D-n9**, **3D-n10**, and **3D-n11** can be easily obtained by rotating in a concerted movement some square blocks or lines of square blocks.

All of the next four nets (**3D-n12**, **3D-n13**, **3D-n14**, and **3D-n15**) are different combinations of the A and E blocks. **3D-n12** and **3D-n13** were first obtained from the 6(3)3-26 net of ref 17, the other two just observing that it was possible to combine the A and E blocks in two other ways. These nets are closely related to the **2D-n1** and **2D-n2**, since they are assembled using the same kind of building blocks.

The last net we present here is **3D-n16**. It is built using the building block 19, and it is strictly related to the **2D-n8** net. The projections along the *a* and *b* axes show the same pattern as **2D-p2**, as we expect. Along the *c* axis the pattern

is the same as **2D-n3**, and a closer look at **3D-n16** shows that this net is also the 3D expansion of **2D-n3**.

### What We Do Not Have

Until now, we have described what we obtain applying the *topochemical* constraint to the 3-coordinated nets. Here we want to show what one cannot build.

First of all one cannot make a zero-dimensional solid with all T-shape points. In 3-coordinated polyhedra, such as the cube or the tetrahedron, the neighbors to a vertex do not lie in one plane with the vertex, as for the T-shape.

We spent some time in trying to build a T-shape net formed only by lines with three points in a row. The reasons for our interest in such a net will be clear in the next section. The lack of this kind of net is related to the characteristic of the three-atomic line. From our attempts to build such a net, it emerges that we have an abundance of linkages at the ends of the lines and a shortage of link points in the middle of the lines. This is obviously related to the fact that there are 2 points at the ends of the lines for each central point.

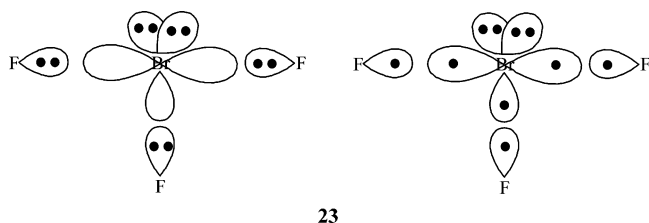
To overcome this difficulty we also tried to build a T-shape dendrimer formed only by three atomic lines. This looks to be impossible using only T-shape building blocks; after a few generations, the dendrimer collapses for lack of space.

Up to here we have had fun (*and a few tears*) with geometry. Now we want to start to populate the nets with atoms and their electrons. To describe the electronic properties of such nets we need to introduce some concepts of the electron counting.

### Electron Counting for T-Shape Nets

**General.** Our aim is to reason out the favored (some would call them “magic”) electron count for every T-shape net. This will be done qualitatively here, followed by a computational analysis for a selected subset of the nets in a subsequent paper.

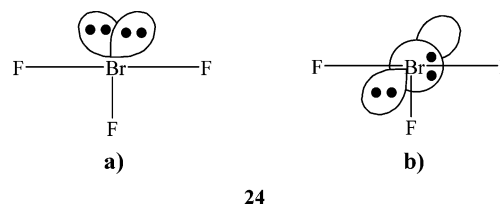
The molecular prototype for T-shape bonding is the relatively small set of T-shape molecules, such as  $\text{BrF}_3$  and  $\text{ClF}_3$ . These may be described in an ionic or covalent way; at left in **23** is the ionic starting point ( $\text{Br}^{3+}(\text{F}^-)_3$ ), at right the covalent one ( $(\text{Br}^0)(\text{F}^0)_3$ ).



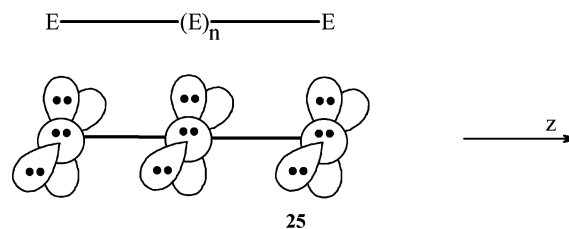
Note the assumption of  $sp^2, p$  hybridization at the Br. The outcome in either case is a “normal” (dative or covalent) Br–F bond along the vertical axis of the T, two lone pairs at Br, and a three-center four-electron bond along the bar of the T.

Actually there is not much s,p mixing in molecules of the right side of the Periodic Table, once one leaves the first

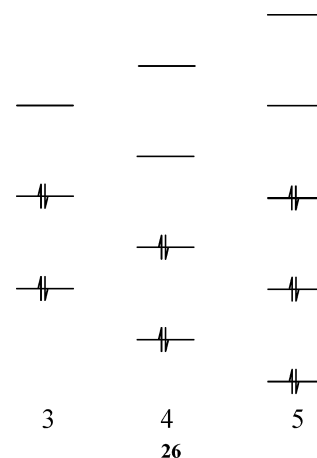
row. So whereas the lone pairs in  $\text{BrF}_3$  might be represented either as **24a** or **24b**, as one goes down the Periodic Table, the s,p representation **24b** is increasingly more appropriate.



Structural motifs which occur in our nets are not only the T-shape but also, commonly, an infinite linear chain, as well as finite linear chains 3, 4, 5, 6, ... atoms long. The electronic structure of these has been analyzed elsewhere,<sup>7</sup> but let us review the argument here. Consider a chain of any length, symbolically indicated in **25**. Under the assumption of little s,p-mixing, each atom in the chain can be assigned 6 electrons to begin with, two each in  $np_x$ ,  $np_y$ , and two in  $ns$  orbitals.



There remains the  $np_z$  orbital set. In **26**, we indicate the orbital pattern (Hückel-type) of chains of length 3, 4, and 5.



We’ve learned that “thou shall not fill antibonding levels” is not a bad guide for stability. This leads to a “good” electron count of 4 for 3 orbitals, 4 for 4 orbitals, 6 for 5 orbitals, etc. Or, in general,  $n + 1$  for  $n = \text{odd}$ ,  $n$  for  $n = \text{even}$  (where  $n$  is the number of atoms). We can also express this result in another way (this will be useful soon). The number of electrons optimizing bonding *per atom* in the direction of a line of  $n$  main group atoms is 1 if  $n$  is an even number and  $1 + 1/n$  if  $n$  is odd.

For the infinite system half of the band is filled. When one adds these  $n$  (or  $n + 1$ ) electrons to the  $6n$  in the  $ns$  and

## Main Group Element Nets to a T

$p_{x,y}$  set, one comes to a preferred electron count of 7 per main group element atom in the infinite linear chain. Or to put into a tabular form we will find useful, per atom the following occupation numbers are best (27) for an infinite linear chain.

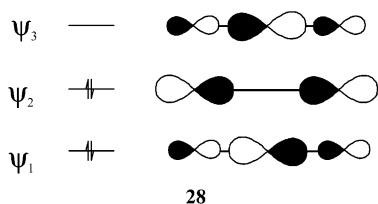
	s	$p_x$	$p_y$	$p_z$
occupation number	2	2	2	1

27

We will also need for our *Aufbau* one- and two-atom fragments. For a singly bonded diatomic, we'd need 2 electrons along  $p_z$  for 2 atoms. For a single atom, we have a lone pair and a filled octet. In this way we make a connection between electron-rich bonding with electron-precise bonding.

One further essential concern needs to be discussed. While the favored electron count per atom is 7 for the infinite chain, and the same for every atom in the chain, what about the distribution of electrons in the finite chain? Or to put it another way,  $I_3^-$  (the prototype  $n = 3$  system) has 22 valence electrons. How are they distributed?

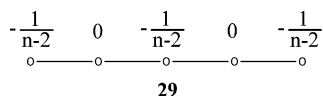
Consider the four electrons of  $I_3^-$  in the  $np_z$  set, 28.



In a Hückel calculation  $\psi_1 = \frac{1}{2}(\chi_1 - \sqrt{2}\chi_2 + \chi_3)$  and  $\psi_2 = \sqrt{\frac{1}{2}}(\chi_1 - \chi_3)$ . Thus the electron distribution in  $\psi_1$  is 0.5, 1.0, 0.5 along the chain, and in  $\psi_2$  1.0, 0.0, 1.0. The sum (1.5, 1.0, 1.5 along the chain) places a  $-1/2$  negative charge at the ends of the chain.

Is this real? Sort of. If one does an extended Hückel calculation<sup>19</sup> in  $I_3^-$ , one obtains charges of (-0.54, 0.08, -0.54) along the chain. Better calculations give (-0.45, -0.10, -0.45).<sup>20</sup> Clearly this is an approximation on the way to reality.

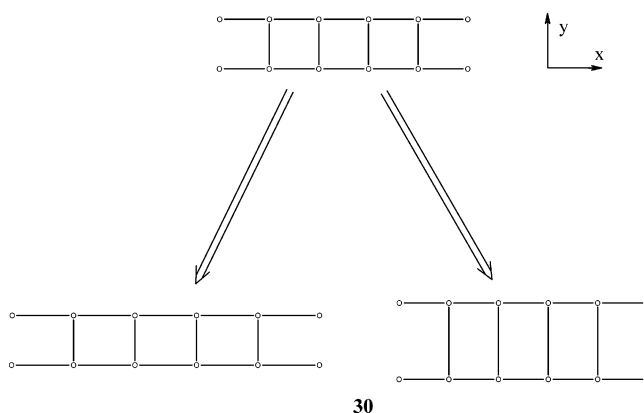
The Hückel treatment of a general odd-membered orbital system places negative charges of  $-[1/(n - 2)]$  on every other atom, starting from the end, as in 29. For even-membered chains with  $n$  electrons the atoms are uncharged.



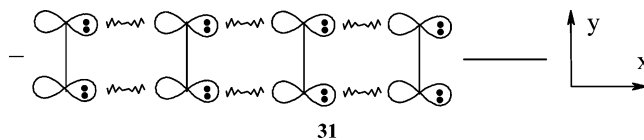
In summary, the optimal electron count depends on the length of the atom lines in the net. Chains with an even or infinite number of atoms have one electron per atom in that direction, while chains with an odd number have an electron count of  $1 + 1/n$  per atom where  $n$  is the number of atoms of

the chain. A consequence is that nets with links with only even or infinite chains have a favored electron count per atom of six. Also the highest theoretical electron count possible for the T-shape nets is  $6 + 2/3$ . This will correspond to a net formed only by triatomic lines, a net that we found impossible to construct. In general the electron count will be in the range 6 (included) to  $6 + 2/3$ . We are now ready to analyze some specific systems, again climbing a ladder of dimensionality.

**Electron Counting: A 1D Ladder.** Infinite linear chains of atoms and pair fragments form the ladder. So its electron count is six, but let us obtain the optimum electron count for the ladder in a different way. The approach we use is to “retrotheoretically” decompose the ladder into smaller pieces.<sup>21</sup> For these building blocks we know the electron count, and the process can then be reversed; we will call this an *Aufbau*. Two possible retrotheoretical ways are shown in 30 for the simple ladder. In the first case, we break the ladder in steps, in the second to lines.



We begin with the *Aufbau* from pairs, really diatomic molecules. The molecular model might be singly-bonded  $I_2$ . So the electron count per atom is 7 electrons. Consider approaching such 7 electron diatomics so as to form the ladder, as 31 indicates; one should then get only repulsion from the lone pairs impacting on each other. Optimum bonding can be achieved by oxidizing each  $p_x$  lone pair by one electron. So the final electron count per atom is 6 electrons.



We can also break the ladder into two linear chains. As we saw, the best electron count per atom of a linear chain is 7 electrons. Bringing two such lines up to each other (32), one would encounter repulsion, as shown in 32, now between two  $p_y$  lone pairs. To form the bond we have to oxidize each  $p_y$  lone pair by one electron. Thus, as in the previous case,

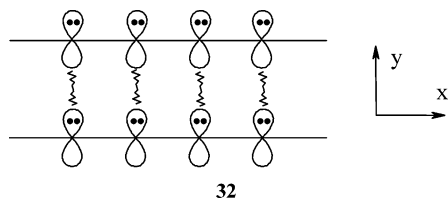
(19) (a) Hoffmann, R.; Lipscomb, W. N. *J. Chem. Phys.* **1962**, *36*, 2872.

(b) Hoffmann, R.; Lipscomb, W. N. *J. Chem. Phys.* **1962**, *37*, 3489.

(20) For the calculation we used the hybrid DFT method (B3LYP) and the lan12dz basis set with the corresponding electron core potential.

(21) Ienco, A.; Papoian, G. A.; Hoffmann, R. *J. Am. Chem. Soc.* **2001**, *123*, 2317.

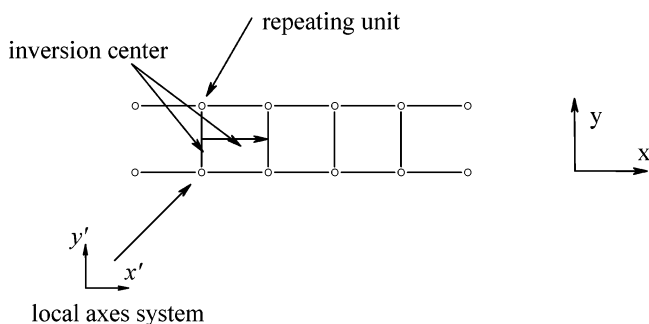
the predicted electron count for the ladder is 6 electrons per atoms.



32

The procedure detailed above is instructive. It indicates that there may be different ways of fragmentation, and that each way can be informative as to the electronic structure of the net. On the other hand, the *Aufbau* outlined is system-specific. Because we have to deal with a large number of structures, we develop below an analytical method that is more systematic.

First of all, we identify the repeating unit of the ladder. This is the diatomic molecule, as shown in 31. We also notice that the two atoms in the diatomic molecule are equivalent by symmetry. An inversion point relates them.



33

So we have to analyze only one atom. Let us first define a local axis system for the atom, indicated in 33 as  $x'$  and  $y'$ . The  $x'$  axis is chosen parallel to the vertical part of the T, and the  $y'$  axis along the bar of the T. One reasonable assumption, as we mentioned above, for late main group element nets is that there is no s,p mixing in them. We assign a full two electrons to the s orbitals. Next we have to decide how many electrons to assign to the various p orbitals.

Each atom belongs to a straight line in the x direction, to a line of two elements in the y direction, and has no neighbor in the z direction. The corresponding electron counts optimizing bonding are 1 electron for the  $p_{x'}$  and the  $p_{y'}$  orbitals and 2 electrons in the  $p_{z'}$  orbitals. This is shown in tabular form in 34. In total, the electron count per atom is 6 electrons.

	s	$p_{x'}$	$p_{y'}$	$p_{z'}$	total
occupation number	2	1	1	2	6

34

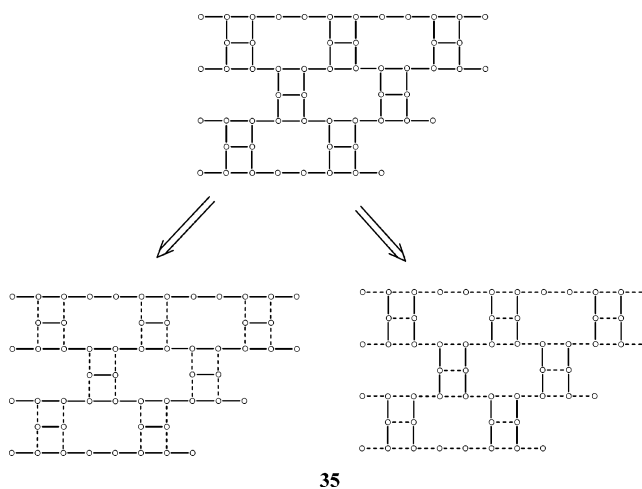
In general, to obtain the electron count ( $EC_{\text{net}}$ ) per atom of the net, the electron count of each atom ( $EC_i$ ) has to be multiplied by the multiplicity of the atom in the unit cell ( $m_i$ ) and divided by the total number of atoms in the unit cell ( $n_{\text{tot}}$ ) as shown in eq 4.

**Table 2.** Some Topological and Electronic Properties of the Planar 2D Nets

net	symbol	electron count	lines
<b>2D-p1</b>	(4.8, 3)	6	4
<b>2D-p2</b>	(4 <sup>2</sup> .10, 3)-a	$6 + \frac{1}{3}$	$\infty, 3, 2$
<b>2D-p3</b>	(4 <sup>3</sup> .12, 3)-a	6	$\infty, 4, 2$
<b>2D-p4</b>	(4 <sup>4</sup> .14, 3)-a	$6 + \frac{1}{5}$	$\infty, 5, 2$
<b>2D-p5</b>	(4 <sup>5</sup> .16, 3)-a	6	$\infty, 6, 2$
<b>2D-p6</b>	(4 <sup>2</sup> .10, 3)-b	6	6, 4, 2
<b>2D-p7</b>	(4 <sup>3</sup> .12, 3)-b	6	8, 4, 2
<b>2D-p8</b>	(4 <sup>4</sup> .14, 3)-b	6	10, 4, 2
<b>2D-p9</b>	(4 <sup>5</sup> .16, 3)-b	6	12, 4, 2
<b>2D-p10</b>	(4 <sup>3</sup> .8.10, 3)	$6 + \frac{1}{5}$	5, 4, 2
<b>2D-p11</b>	(4 <sup>4</sup> .8.12, 3)	$6 + \frac{1}{3}$	5, 2

$$EC_{\text{net}} = \frac{\sum_{i=1}^{n_{\text{tot}}} (m_i EC_i)}{n_{\text{tot}}} \quad (4)$$

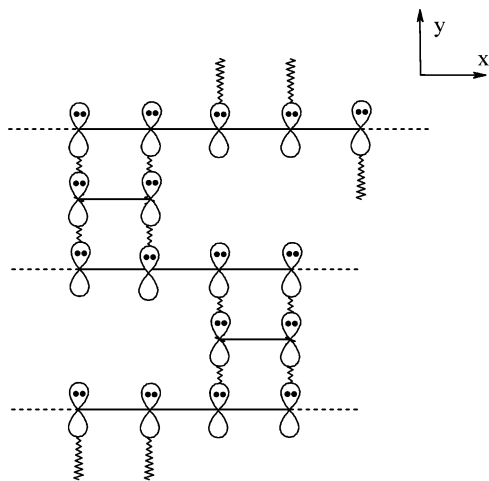
**Electron Counting: 2D Planar Nets.** The optimal electron count for the various planar 2D nets is given in Table 2. Most of them have an electron count of 6 electrons, as the number of atoms of all chains in the nets is even or infinite. Before proceeding, we want to analyze in detail a case which does not give an electron count of 6 electrons. So we choose the **2D-p2** net. Its retrotheoretical decomposition is shown in 35.



35

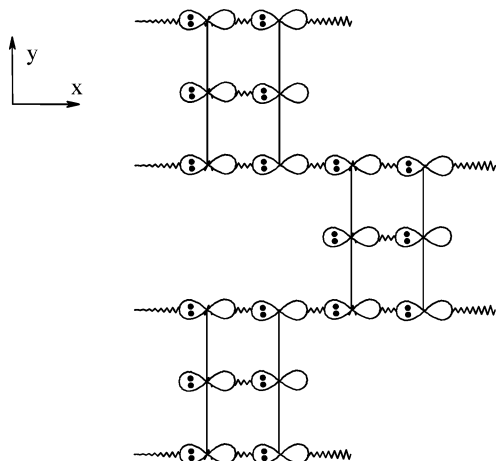
As we did for the ladder, we want to analyze two different ways of cutting the net. In the left side of 35, the decomposition leads to a series of linear infinite chains and pairs of atoms, in the right side only triatomic units. In the first case, the electron count for the infinite lines and for the diatomic units is 7. When we construct the net by bringing the fragments together, for each triatomic link formed, we have 3 orbitals filled by 6 electrons (see 36). To minimize repulsion, we need to remove 2 electrons for each triatomic link, or  $\frac{2}{3}$  electron per atom. So the final electron count per atom is  $7 - \frac{2}{3}$  or  $6 + \frac{1}{3}$ .

For the other decomposition, the model for the triatomic molecule is  $I_3^-$  with an electron count per atom of  $7 + \frac{1}{3}$ . In this case we form two different types of linkages, a single bond and an infinite chain. To form the bonds in both cases,



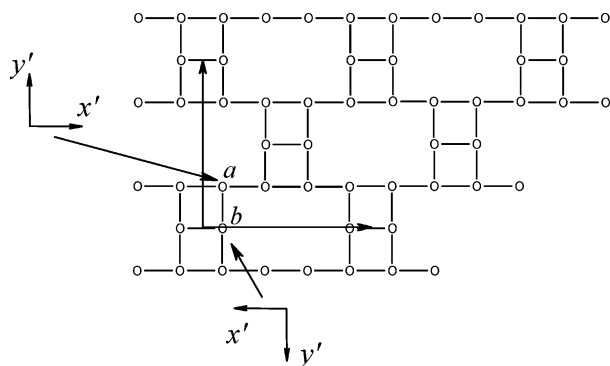
36

one electron for each  $p_x$  orbital has to be removed (see 37). So the final electron count per atom is again  $6 + \frac{1}{3}$ .



37

We also want to illustrate how to obtain the electron count using the analytical method. The unit cell for the **2D-p2** is shown in 38.



38

The planar group is  $c2mm$ , and in the unit cell there are 12 atoms. There are 2 types of atoms. The first one, “a”, is on the linear chain with a multiplicity of 8, and the second one, “b”, is in the middle point of the triatomic line with a multiplicity of 4. To calculate the electron count we use the atoms indicated in 38. Notice also how the local Cartesian

axes are differently oriented with respect to the unit cell axes, as a consequence of the different orientation of the T.

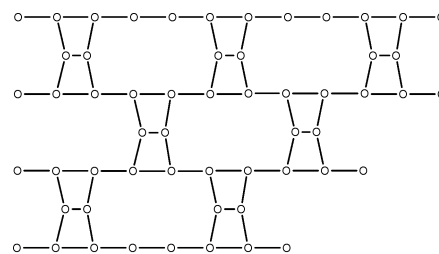
As shown in 39, the  $s$  and  $p_z$  orbitals of “a” host 2 electrons each (lone pairs), and the  $p_x$  orbital, located on the linear infinite chain, has 1 electron. The  $p_y$  orbital is on one terminal of the triatomic line, and so it is filled optimally with  $1 + \frac{1}{3}$  electrons. For the point “b”, the  $x$  direction is along the triatomic line, so the  $p_x$  orbital has  $1 + \frac{1}{3}$  electrons, while the  $p_y$  is filled with only one electron (the electron count for a pair of atoms). Applying eq 4, we obtain again an electron count per atom of  $6 + \frac{1}{3}$ .

atom type	multiplicity	s	$p_x$	$p_y$	$p_z$	total
a	8	2	1	$1 + \frac{1}{3}$	2	$6 + \frac{1}{3}$
b	4	2	$1 + \frac{1}{3}$	1	2	$6 + \frac{1}{3}$

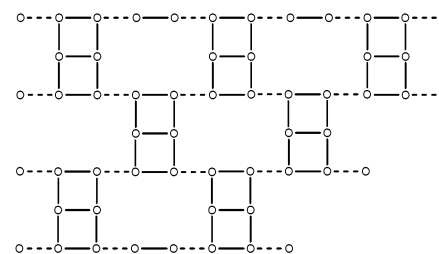
$$EC_{2D-p2} = \frac{8(6 + \frac{1}{3}) + 4(6 + \frac{1}{3})}{12}$$

39

This net may well deform. The bond between two adjacent atoms of type “b” is single, so it is stronger with respect to the corresponding bonds in the linear chain and it will try to form a shorter bond. This may lead to a trapezoidal structure (see 40a) or to a series of rectangular units (see 40b). The same problem may also be common for the other 2D nets of the same family (**2D-p3**, **2D-p4**, **2D-p5**, ..., etc.), as well as in the other nets, when a single bond is close and parallel to a hypervalent linkage. On the contrary, the **2D-p1** net seems not to be affected by a deformation as in 40a; all the bonds are symmetry equivalent, but an elongation of the inter-square with respect to the square bonds can occur.



a)



b)

40

A more detailed analysis of the problem will be presented separately. We now want to introduce the electron counting for the nonplanar nets.

**Electron Counting: Nonplanar Nets.** Table 3 shows the electron count for the nonplanar nets. The highest electron

**Table 3.** Some Topological and Electronic Proprieties of the Nonplanar Nets

net	type	electron count	lines
<b>1D-n1</b>	binodal	$6 + \frac{1}{3}$	$\infty, 3, 2$
<b>1D-n2</b>	trinodal	$6 + \frac{1}{4}$	$\infty, 3, 2$
<b>2D-n1</b>	binodal nonlayered	6	$\infty, 4, 2$
<b>2D-n2</b>	binodal nonlayered	6	$\infty, 4, 2$
<b>2D-n3</b>	trinodal	$6 + \frac{3}{10}$	$\infty, 3, 2$
<b>2D-n4</b>	binodal	$6 + \frac{3}{10}$	5, 2
<b>2D-n5</b>	same as <b>2D-n4</b>	$6 + \frac{3}{10}$	5, 2
<b>2D-n6</b>	trinodal	$6 + \frac{1}{4}$	$\infty, 3, 2$
<b>2D-n7</b>	tetranodal	$6 + \frac{1}{2}$	5, 3
<b>2D-n8</b>	hexanodal	$6 + \frac{3}{7}$	$\infty, 3, 2$
<b>2D-n9</b>	decanodal	$6 + \frac{2}{5}$	$\infty, 3, 2$
<b>3D-n1</b>	ThSi <sub>2</sub>	6	$\infty, 2$
<b>3D-n2</b>	B <sub>2</sub> O <sub>3</sub>	6	$\infty, 2$
<b>3D-n3</b>	6.6.14 <sub>3</sub>	6	$\infty, 2$
<b>3D-n4</b>	4.12 <sub>2</sub> .12 <sub>2</sub>	6	4
<b>3D-n5</b>	trinodal	$6 + \frac{1}{4}$	$\infty, 3, 2$
<b>3D-n6</b>	same as <b>3D-n5</b>	$6 + \frac{1}{4}$	$\infty, 3, 2$
<b>3D-n7</b>	SrSi <sub>2</sub>	$6 + \frac{1}{4}$	$\infty, 3, 2$
<b>3D-n8</b>	trinodal	$6 + \frac{1}{4}$	$\infty, 3, 2$
<b>3D-n9</b>	binodal	$6 + \frac{1}{2}$	$\infty, 3$
<b>3D-n10</b>	binodal	$6 + \frac{1}{2}$	$\infty, 3$
<b>3D-n11</b>	trinodal	$6 + \frac{1}{3}$	$\infty, 4, 3$
<b>3D-n12</b>	binodal	6	$\infty, 4, 2$
<b>3D-n13</b>	same as <b>3D-n12</b>	6	$\infty, 4, 2$
<b>3D-n14</b>	trinodal	6	$\infty, 4, 2$
<b>3D-n15</b>	trinodal	6	$\infty, 4, 2$
<b>3D-n16</b>	trinodal	$6 + \frac{3}{7}$	$\infty, 3, 2$

count we have is  $6 + \frac{1}{2}$  for **2D-n7**, **3D-n9**, **3D-n10**. These nets share interesting features, such as the presence of a high number of squares. And they are obviously related. The **2D-n8** and **3D-n16** nets have a slightly lower electron count ( $6 + \frac{3}{7}$  or 6.43). Their strictly related **2D-n9** net has an electron count of 6.40 while the **2D-n3** net is lower due the higher number of straight lines.

In general, nets with similar geometric characteristics and formed by the same kind of building blocks have equal

electron count. This is true for the series **3D-n1**, **3D-n2**, and **3D-n3** (all the latter have linear chains connected together) as well as for **2D-n1**, **2D-n2**, **3D-n12**, **3D-n13**, **3D-n14**, and **3D-n15** (again linear chains connected by the E building block). Interestingly, we can also make a relationship between the **1D-n2** and the **2D-n6**, **3D-n5**, **3D-n6**, **3D-n7**, and **3D-n8**. They are built using linear chains and building block D. In contrast, there are no evident common features between **2D-n3** and conformers **2D-n4** and **2D-n5**. Also the **3D-n11** net is unique, while the **1D-n1** net is obviously related with its parent **2D-p2**.

### Concluding Remark

With this we end the first step in a fascinating geometrical and electronic journey through T-shape nets. The geometries we generate may be used to classify linker-spaced molecular nets that do exist. These nets, however, are not necessarily subject to the topochemical constraint we have imposed in our enumeration. So they may show additional topologies. No examples of such nets entirely composed of main group atoms exist. Yet.

**Acknowledgment.** We are grateful to the National Science Foundation for its support of this research through Grant CHE02-04841.

**Supporting Information Available:** In this section, we report the space group, the cell constant, the crystallographic coordinates, the density as well as the vertex symbol for all the 38 nets (2D and 3D) described here. The demonstration of the uniqueness of the net **2D-p1** is also given. Also a text file with the space groups and the coordinates of the nets is also included to allow the reader to import and visualize easily the structures into a structure drawing program. This material is available free of charge via the Internet at <http://pubs.acs.org>.

IC0353211